P2.5 # SOURCE MODELING OF MICROBAROMS IN THE PACIFIC

Mark C. Willis*, M. Garces, C. Hetzer, and S. Businger.
SOEST, University of Hawai'i at Manoa, Honolulu, Hawai'i

1. Introduction

Infrasound consists of low frequency sound waves that are below the 20 Hz hearing threshold of the human ear. Due to low atmospheric absorption at low frequencies, infrasonic waves can propagate thousands of kilometers and can be readily detected by surface based instruments. Naturally occurring sources of infrasound include (but are not limited to) severe weather, volcanoes, bolides, earthquakes, surf, mountain waves, and, the focus of this research, nonlinear open ocean wave interactions.

The International Monitoring System (IMS) was organized under the Comprehensive Nuclear Test Ban Treaty to continuously monitor the Earth for nuclear test explosions. Signals observed at IMS infrasound station I59US, Hawaii, are studied to characterize the background noise field. Much of this background noise is related to pervasive signals known as microbaroms. Microbaroms consist of atmospheric pressure fluctuations with energy between 0.1 and 0.5 Hz that can appear as coherent energy bursts or as a continuous oscillation. For infrasonic stations near the ocean, microbarom clutter often completely defines the low-wind noise floor. The microbarom peak is in the midst of the detection region for 1kt nuclear explosion tests. Microbaroms can therefore make it difficult to study a signal of interest.

Microbaroms were first observed by Benioff and Gutenberg (1939) on an electromagnetic barograph and they hypothesized that these signals were the result of low pressure systems in the Northeast Pacific Ocean. Further studies confirmed that the microbarom source is related to severe weather in the ocean and the resulting high ocean surface waves (Saxer, 1954, Daniels, 1962, Donn and Posmentier, 1967 Rind, 1980). These early studies relate microbarom arrivals to major weather patterns, especially to cold frontal systems and low pressure centers, and their associated regions of high ocean surface waves.

Microseisms are attributed the same source processes as microbaroms, but the former propagate in the ground and oceans. Longuet-Higgins (1950) described a mechanism for the source generation of microseisms involving the interaction of standing ocean waves with the sea floor. The confirmation that microbaroms and microseisms share the same source was made by Donn and Posmentier (1967), Donn & Naini (1973) and again by Rind (1980). Arendt and Fritts (2000) presented an acoustic source pressure formulation based on the Longuet-Higgins method. They found that two ocean surface gravity waves can radiate propagating acoustic waves if the two ocean waves are propagating at nearly equal but opposite directions with similar frequencies. In this research the theoretical microbarom generation model of Arendt and Fritts (2000) and global wave spectra from the third-generation Wavewatch 3 (WW3) ocean wave model of Tolman (1999) are used to predict acoustic source pressure spectra.

2. Data, Methods and Instrumentation

Infrasound station I59US is part of the global infrasound network of the International Monitoring System (Vivas-Veloso et al., 2002). The Hawaii station has very low ambient noise levels and is one of the most sensitive stations of the IMS because of its location in a dense tropical forest and leeward of massive volcanoes. The station consists of four Chaparral 5 microphones with a passband of 0.05-8 Hz and a dynamic range exceeding 120 dB. Three of the sensors are arranged as a triangle with a 2km baseline, with the fourth sensor near the center of the triangle. Sensor data are recorded by 24-bit digitizers and sent in real time via radio telemetry to the Infrasound Laboratory in Keahole Point, West Hawaii. The PMCC algorithm of Cansi et al. (1995) is used to detect coherent infrasonic energy across the array and extract the speed, arrival angle, and amplitude of the detected arrivals.

The WW3 ocean wave model (v1.18) which is driven by NOGAPS 10m surface winds and global ice concentration values is used to produce realistic ocean wave spectra values on a global 1-degree grid. For all case studies WW3 is initialized at least 6 days ahead of noteworthy events to allow for proper growth and dispersion. WW3 outputs spectra at every grid point in the form of wave energy densities in 24 directional and 25 frequency bins. These wave spectra are then used to calculate acoustic source pressure by summing the products of directly opposing wave trains at each frequency.

* *Corresponding author address:* Mark C. Willis, Univ. of Hawaii at Manoa, Dept. of Meteorology, 2525 Correa Rd. Honolulu, HI 96825; e-mail: mwillis@hawaii.edu

Observational and modeling results are shown for January 4, 2003 at which time seven surface low pressure centers were evident in the Pacific Basin, including an intense (sub 952mb) and symmetrical mid latitude cyclone that was moving east-northeastward just north of the Hawaiian Islands. Surface pressure charts for this case were generated using data supplied by the NCEP/NCAR Reanalysis project which is available in 6 hourly intervals at a resolution of 2.5°. Microbarom arrival azimuths at IS59 are compared to location of Pacific basin low pressure centers and significant wave heights produced by WW3. Azimuthal detection of infrasound arrival is determined by finding the best correlation between waveforms on the elements of the array, determining timeshifts that would be necessary to cause waveforms to line up best, and calculating the azimuth from which the waves would have to be arriving from in order to achieve those timeshifts. These are referred to as coherent arrivals. Infrasonic power spectral densities are used to distinguish peaks in the microbarom frequency range. Power spectra include the combination of both coherent and non-coherent microbaroms at IS59 at each frequency.

Infrasonic arrays will detect sound waves from the largest and closest sources. Low pressure systems, acoustic source pressure peaks and minima are thereby studied for the Pacific Basin only due to the abundance of acoustic energy created by ocean waves in the Pacific at any given time. Sources outside of the Pacific are considered negligible.

3. Microbarom Observations

Microbarom arrival azimuths at IS59 during 2002 show an annual cycle (Fig. 1). During the months from June through September arrivals generally come from east (55-130°) or south (160-220°) directions. The concentration of east arrivals is much stronger than the south arrivals during this time. Months October through March show an abundance of arrivals from 230-360° with a peak from northwesterly directions. Arrivals during April, May, late September and early October appear to arrive from a variety of different azimuths with no distinct peak noted.

Arrivals from Jan. 1-3, 2003 are highly concentrated between 270-330° (Fig. 2), consistent with surface low pressure systems in the region during that time. Of particular interest are arrivals from Jan. 4-6, 2003. Peak microbarom signals on the 4th came from northwest azimuths. The arrival peak then rotated clockwise through the 5th when several arrivals from the northeast were evident. Coherent energy from both west and northeast directions was then recorded on the 6th. A sub 952mb middle latitude cyclone was just northwest of Hawaii on the 4th and then moved northeast of IS59 on the 5th (Fig. 3), similar to the directions the microbaroms were coming from. This is the same system that produced massive NW swells for exposed Hawaiian Island shores on Jan. 5-6, 2003 with breakers observed greater than 12m.

On Jan. 4, 2003 18Z seven surface low pressure centers are seen in the Pacific Ocean and its nearby waters (Fig. 4). Each of these has an associated peak in significant wave height (Fig. 5) that is located where pressure gradients are strongest. Four of these lows are in the southern hemisphere but little to no coherent microbaroms from southerly directions were recorded during this time frame.

Infrasonic power spectra on 01/04/18Z (Fig. 7) shows a peak of 0.1 Pa²/Hz near 0.2Hz. A smaller peak of .01 Pa²/Hz is seen near .15Hz. A minimum of less than .001 Pa²/Hz is evident near 0.1Hz. The microbarom peak at 0.2Hz is typical year for most infrasound stations.

4. Source Modeling Results

The following algorithm based on the Arendt and Fritts model was used to predict acoustic source pressure fields on a global 1° grid,

$$P_k^0 = \frac{rcg^2}{4w_m}\left[\int_0^{2p} F(k_x,k_y)F(-k_x,-k_y)dq\right] = \frac{rcg^2}{4w_m}Q_m^0 \quad (1)$$

$$Q_m^0 = \int_0^{2p} F(k_x,k_y)F(-k_x,-k_y)dq = 2\int_0^{p} F(f,q)F(f,q+p)dq \quad (2)$$

where P_k^0 is the acoustic source pressure spectrum, w_m is the microbarom frequency which is assumed to be twice that of the ocean surface waves, r , *c*, and *g* are assumed to be 1 kg m^{-3}, 340 m s^{-2} and 9.81 m s^{-2}, respectively. Q_m^0 contains the product of WW3 produced wave energy densities (F) traveling in opposite directions with frequency held constant, integrated over all 24 directional bins. A detailed derivation of this algorithm is explained in Garces et al. (2003).

Acoustic source pressure calculations show a relationship with storm activity in the Pacific Basin, however there also appears to be a variety of obscure source locations independent of surface weather and wave patterns (Fig. 8). At any given time in the middle of the ocean there may be numerous multidirectional and multi-period swell events (typically more than three but less than 20) passing through a given point – regardless of storm or dominant swell activity in the vicinity. This is best illustrated by comparing the frequency, directional ocean wave spectrum at a Central Pacific location on January 4, 2003 1800Z with surface pressure and significant wave heights at the same time (Fig. 4-6). The wave spectrum at this point (0° N, 153.88° W) shows five different swell peaks arriving at the same time, but weak surface pressure patterns are dominating and no peak in significant wave height is noted. Therefore, there may be opposing wave trains occurring nearly anywhere in the ocean at any given time and the potential for microbarom generation may be widespread.

Six out of seven surface low pressure centers in the Pacific Ocean on 01/04/18Z exhibit a peak in acoustic source pressure at 0.197 Hz just west or southwest of the center of circulation. Lows with a peak in acoustic pressure to the southwest of the center were propagating to the northeast while lows with a peak to the west of the center were propagating more towards the east. The exception is the surface low centered in the extreme NW Pacific (just north of Hokkaido, Japan) where a peak in acoustic pressure is noted to the south of the low center. This storm was propagating almost due north. The acoustic source pressure peak seemingly associated with this low also appears to be much larger and broader than the other peaks. The other interesting finding is the minima in source pressure at 0.197 Hz found in the immediate vicinity of the strong cyclone just NNW of the Hawaiian Islands. The acoustic peak at 0.197 Hz was further upstream of the center in this storm than the others. However, source pressure calculations at smaller frequencies showed a peak closer to this low center (not shown).

4. Conclusions and Discussion

Standing ocean surface waves are created when opposing wave trains of similar frequencies but opposite direction meet. This interaction generates a nonlinear pressure perturbation that is capable of traveling at very high phase velocities and generates an infrasonic wave at the air-sea interface. Modeling of acoustic source pressure suggests that microbaroms do not originate from the center of low pressure areas or necessarily from regions of high amplitude ocean waves. Instead, the probable source location is often upstream of storm propagation direction and more importantly source locations may be independent of surface weather patterns or dominant ocean wave characteristics. This presents a problem that is much more complex than previously appreciated.

Coherent microbarom signals at IS59 generally come from south or east directions during the boreal summer. It is suggested that the arrivals from the south in the boreal summer originate upstream of eastward propagating extratropical storms in the middle latitudes of the southern hemisphere. It is suggested that the east arrivals originate from 1) tropical weather in the East Pacific and 2) trade wind swells reflected from the Hawaiian Island chain. Incident trade wind swells are normally from 50-90° (NE to E) and are very common on the windward beaches of the Hawaiian Islands due to a persistent subtropical anticyclone that dominates the Pacific waters to the northeast much of the year. Sanderson (1993) discussed that northeast to east winds (trades) are present in the Hawaiian Islands from 85 to 95% of the time in summer, and from 50 to 80% of the time in the winter. Reflected swells by a land mass are a function of the incident amplitude and period, along with the steepness and permeability of the coastline (Shore Protection Manual, 1973). The Windward Shores of Hawaii have an abundance of rocky, steep coastline so microbarom generation by reflections is likely. Trade wind swells typically range in period from 8-10 seconds. An incident trade swell from the east with period of 10 seconds interacting with a reflected trade swell from the west would produce an infrasonic wave with frequency 0.2 Hz as explained in the frequency doubling nonlinear interactions of Arendt and Fritts (2000). Microbarom generation by reflections may thus explain part of the common infrasonic spectral peak of 0.2 Hz observed at IS59 throughout the year, especially during summer months.

During the boreal winter, microbaroms arrivals were shown to be concentrated from N and W directions. Arrivals with a northerly component are hypothesized to originate from non-linear interactions of ocean swells generated by eastward moving extratropical storms in the mid-latitudes of the North Pacific. Arrivals from west or west-southwest directions in the boreal winter are likely from Western Pacific tropical cyclones, including those that recurve during extratropical transition. Swell convergence associated with the Intertropical Convergence Zone (ITCZ) can also produce microbarom arrivals at IS59 throughout the year from southeast, south, or southwest directions. Arrivals during fall and spring months were shown to come from a variety of directions with no distinct peak noted, due to the randomness of storm systems in the Pacific Basin during shoulder seasons.

Comparison of microbarom arrivals with surface pressure charts during January 2003 showed a clear relationship between arrival azimuth and storm location. This pattern is consistent throughout the boreal winter due to the close proximity of the storm systems and resulting high ocean surface waves. Arrivals from southern hemisphere sources are less obvious because of the effect of atmospheric conditions along propagation path and the attenuation associated with lengthy propagation paths. The varying atmospheric conditions throughout the year will have a great effect on infrasound propagation path and decay. Incorporation of data from other Pacific IMS stations would allow us to compare arrivals from similar storm systems. This may help confirm that arrivals are actually originating upstream of low pressure systems instead of from the center.

5. Acknowledgements

This research is sponsored by the Army Space and Missile Defense Command under contract No. DTRA01-01-C-0077.

6. References

Arendt, S., and D. Fritts, 2000: Acoustic radiation by ocean surface waves. *J. Fluid Mech.*, **415**, 1-21.

Benioff, H. and B. Gutenberg, 1939: Waves and currents recorded by electromagnetic barographs. *Bull. Am. Met. Soc.*, **20**, 421.

Cansi, Y., 1995: An automatic seismic event processing for detection and location: The P.M.C.C. method. *Geophys. Res. Lett.,* **22**, 1021-1024.

Daniels, F. B., 1952: Acoustical energy generated by the ocean waves. *J. Acoust. Soc. Am*., **24**, 83.
Daniels, F. B., 1962: Generation of infrasound by ocean waves. *J. Acoust. Soc. Am*., **34**, 352-353.
Donn, W. L. and B. Naini, 1973: Sea wave origin of microbaroms and microseisms. *J. Geophys. Res*., **78**, 4482-4488.
Garces, M., C. Hetzer, M. Willis, and S. Businger, 2003: Integration of infrasonic models with ocean wave spectra and atmospheric specifications to produce global estimates of microbarom signal levels. 25th Seismic Research Review, Tucson, AZ.
Gossard, E. and W. Hooke, 1975: *Waves in the atmosphere*. Elsevier Scientific, 283-385.
Jachowski, R. A., Eds., 1973: *Shore Protection Manual*. Volume 1, U. S. Army Coastal Engineering Research Center, 2-110-2-120.
Longuet-Higgins, M. S., 1950a: A theory of the origin of microseisms. *Phil. Trans. R. Soc. Lond.,* **243**, 1-35.
Posmentier, E., 1967: A theory of microbaroms. *Geophys. J. R. Astron. Soc.,* **13**, 487-501.
Rind, D., 1980: Microseisms at Palisades 3. Microseisms and microbaroms. *J. Geophys. Res*., **85**, 4854-4862.
Sanderson, M. Ed., 1993: *Prevailing Trade Winds.* Univ. of Hawaii Press, 12-36.
Saxer, L., 1954: Über Entstehung und Ausbreitung quasiperiodischer Luftdruckschwankungen. *Arch. Meteorol. Geophys. Bioklum*., **A6**, 451-457.
Tolman, H. L., 1999: User manual and system documentation of WAVEWATCH-III version 1.19. NOAA/NWS/NCEP/OMB technical note 166, 110pp.
Vivas Veloso, J., D. Christie, T. Hoffmann, E. Demirovic, P. Campus, M. Bell, A. Molero, A. Langlois, P. Martysevich, J. Carvalho, and A. Kramer, 2002: Status of the IMS Infrasound Network, paper presented at the Infrasound Technology Workshop, De Bilt, Netherlands.

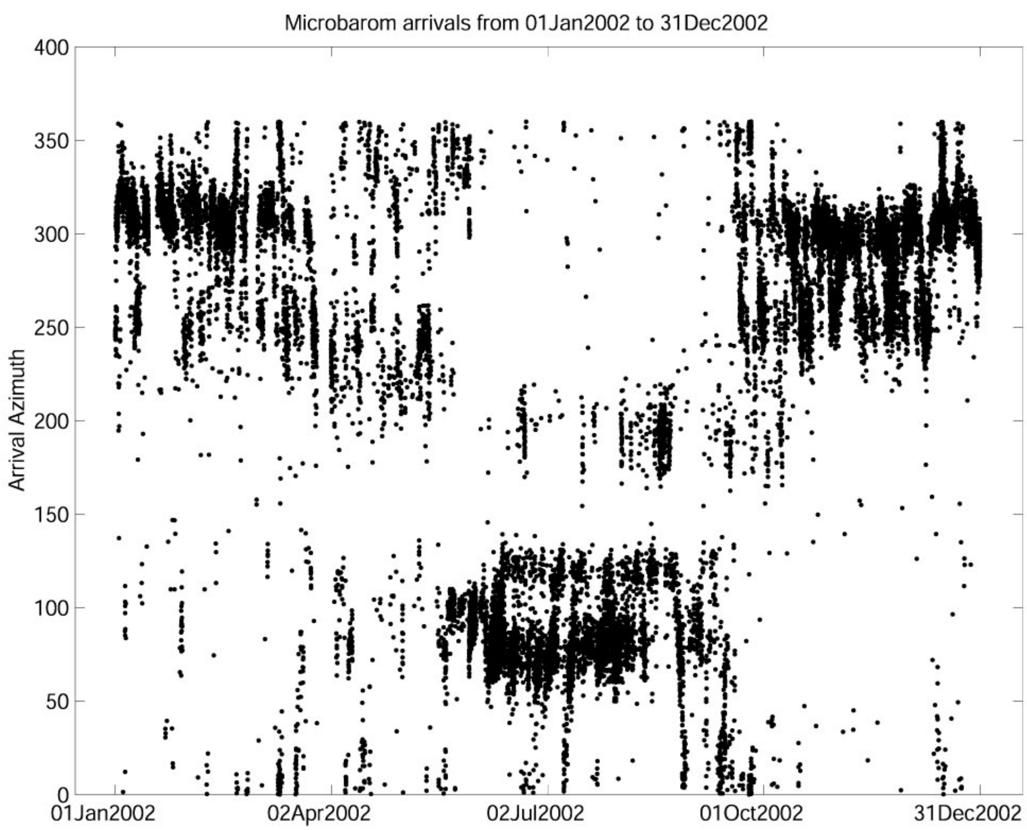

Fig. 1. Time series of coherent microbarom arrivals at I59US for 2002. Arrival azimuth is on the vertical axis going clockwise from north (0° to 360°).

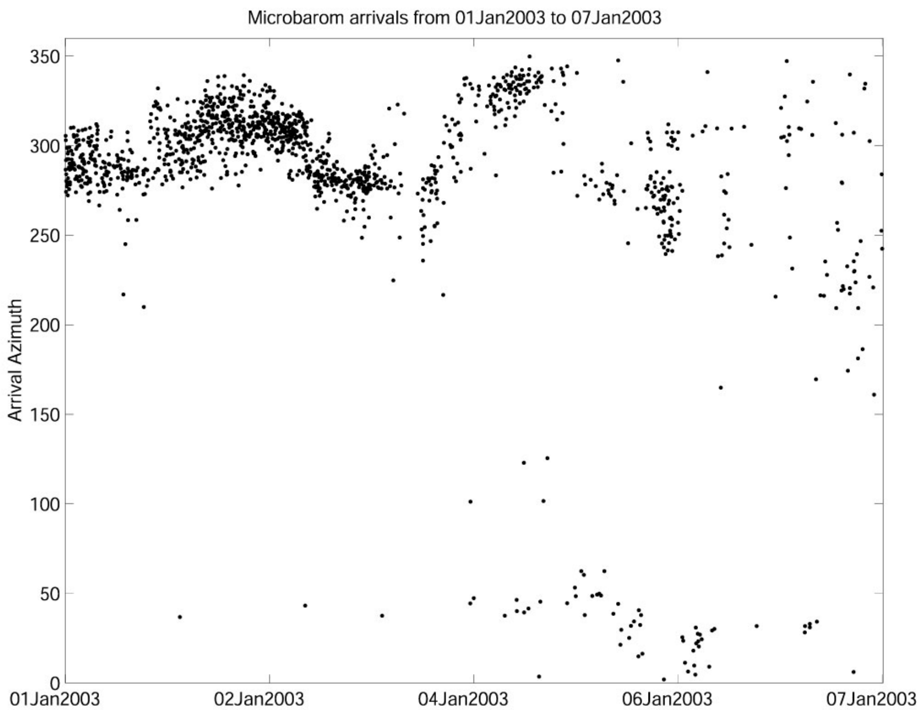

Fig. 2. Arrival azimuth of coherent microbaroms at I59US from January 1-7, 2003.

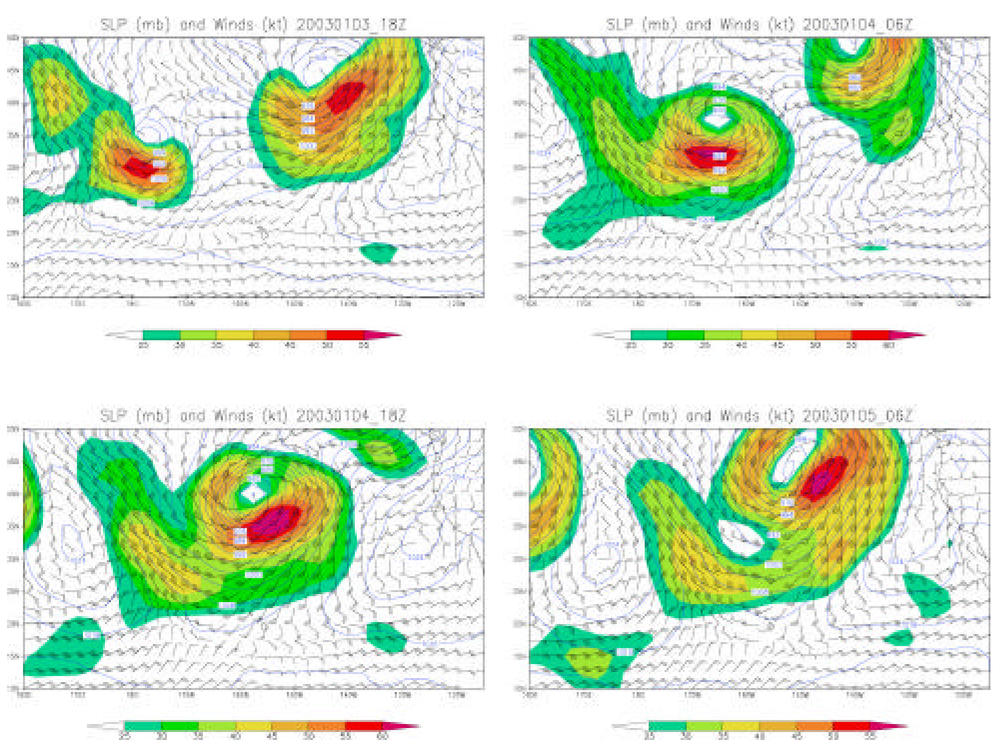

Fig. 3. Analyses of surface pressure (mb) and surface winds (kt) from January 3, 2003 18Z through January 5, 2003 06Z.

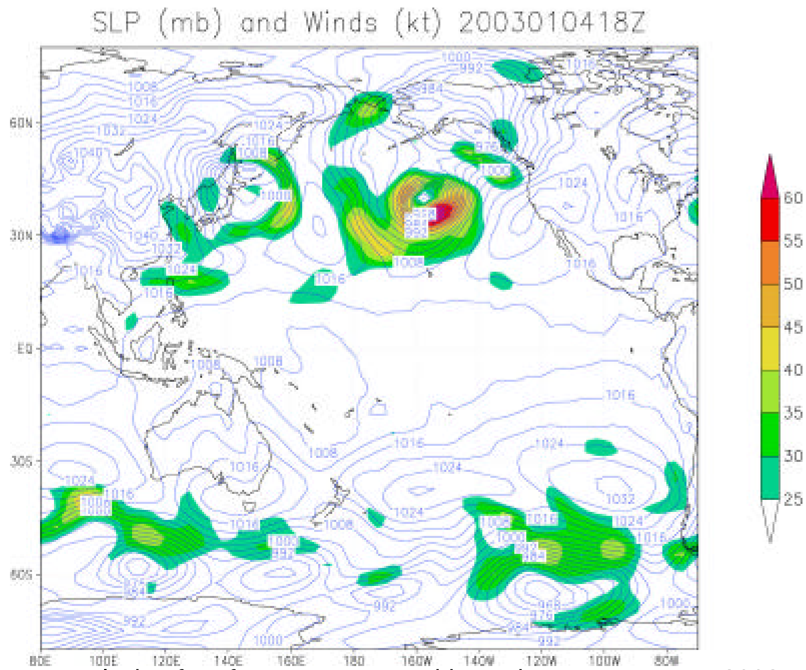

Fig. 4. Analysis of surface pressure and isotachs on January 4, 2003 18Z.

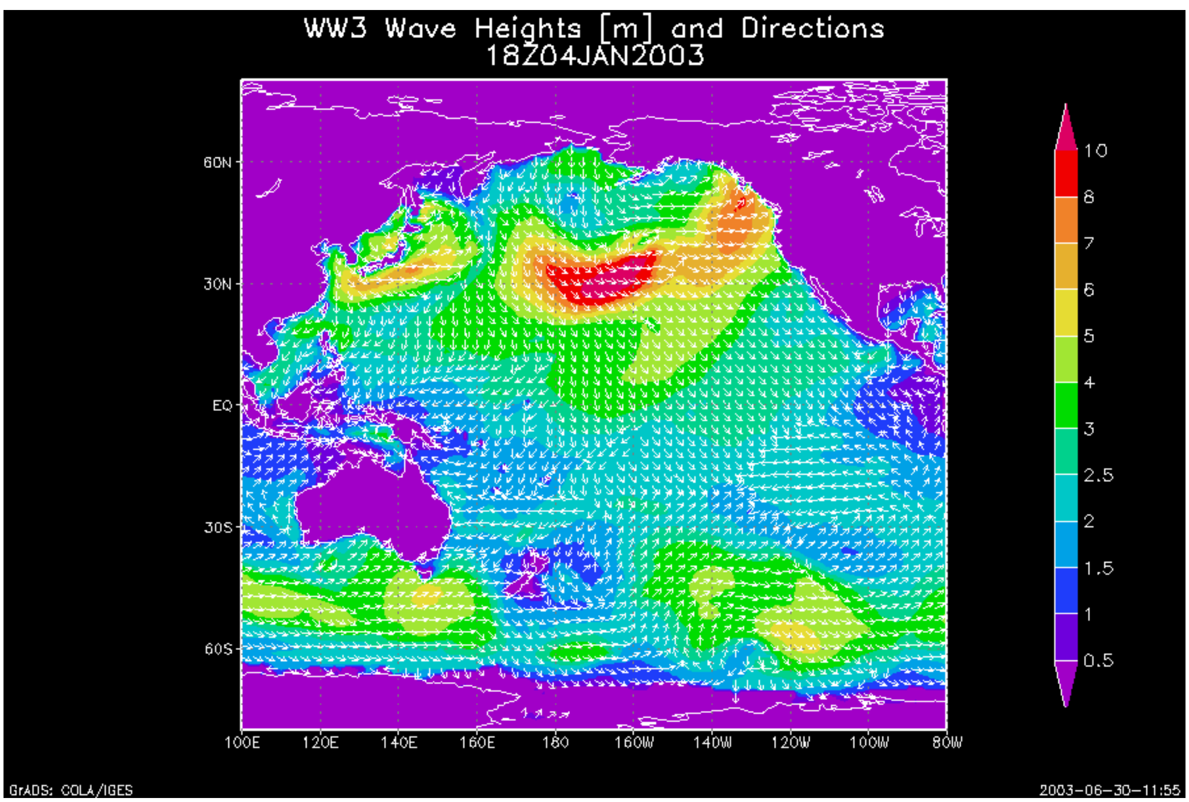

Fig. 5. WW3 Significant wave heights (m) and mean propagation direction vectors (towards) for January 4, 2003 18Z.

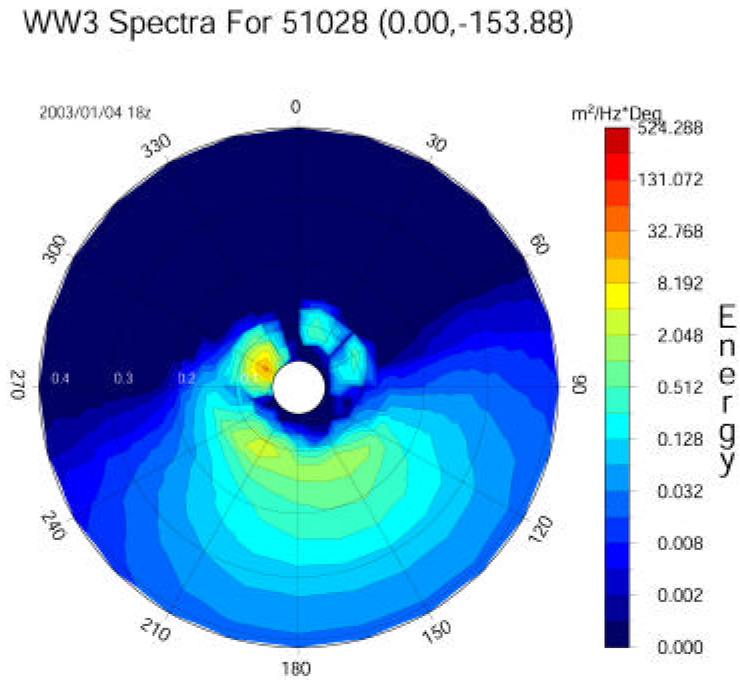

Fig. 6. Frequency, directional ocean wave spectrum for Central Pacific location 0.00N, 153.88W on January 4, 2003 18Z. Frequency (Hz) decreases towards the center, wave energy scale (m²/Hz*Deg) on the right hand side.

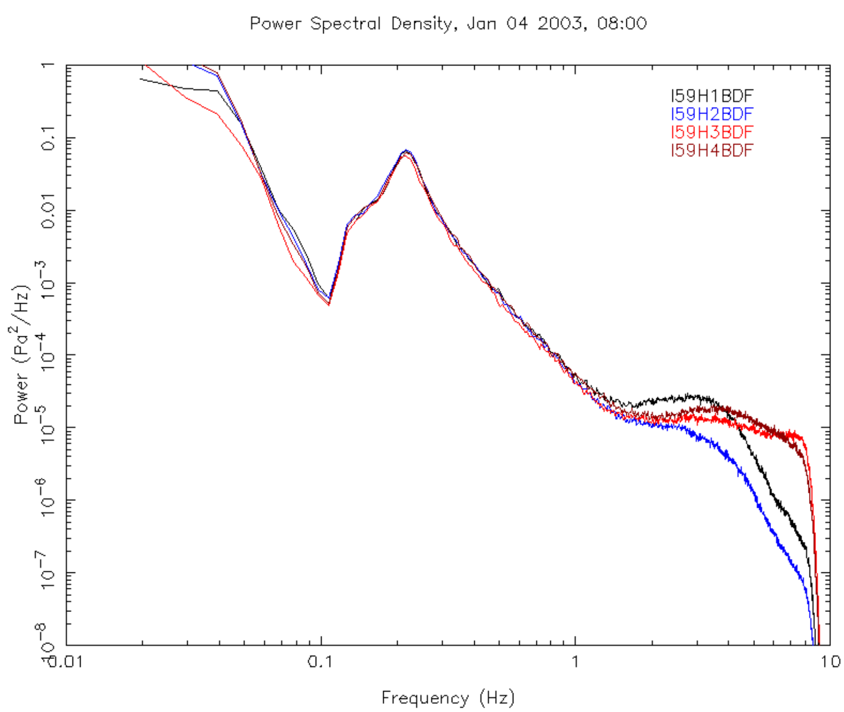

Fig. 7. Acoustic power spectral density observed at IS59 on January 4, 2003 18Z (8am Local). Colored lines represent power observed by the four components of the infrasonic array. Power (Pa²/Hz) is on the vertical axis, acoustic frequency (Hz) is on the horizontal axis.

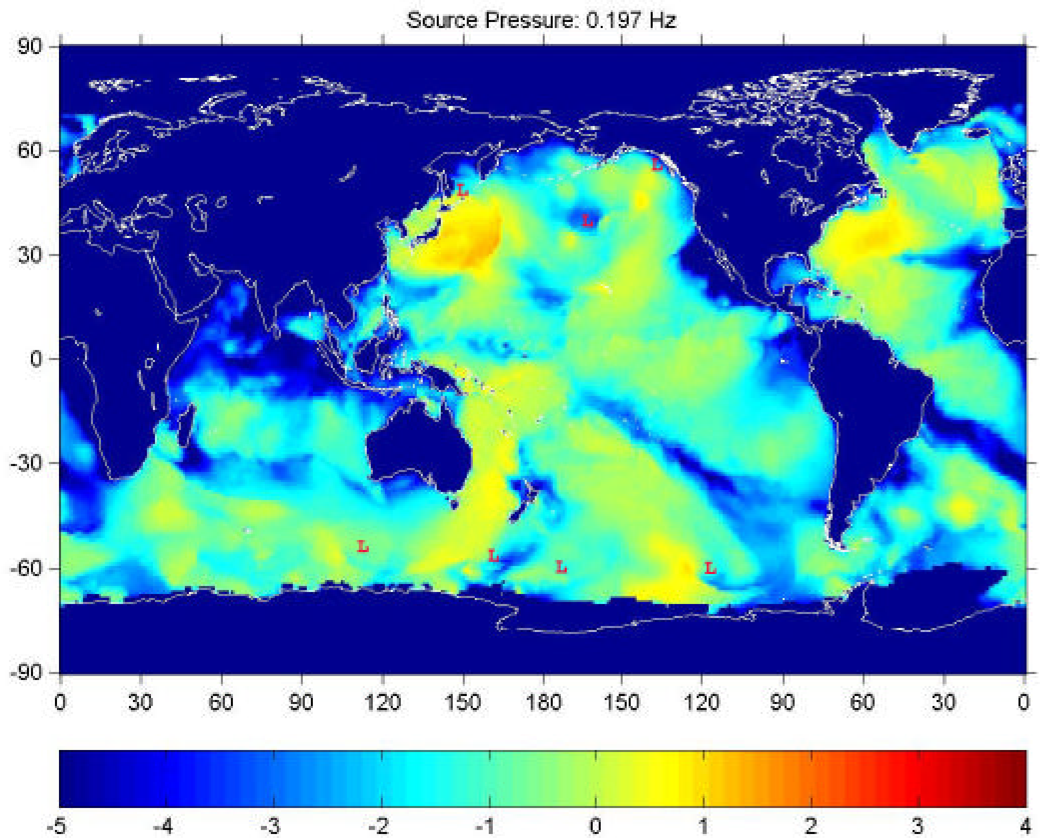

Fig. 8. Base 10 logarithm of acoustic source pressure (Pa * m³) with frequency 0.197 Hz corresponding to ocean waves interacting with periods of ~ 10 s (produced by equation 1 from spectral output given by WW3). Location of surface low-pressure centers indicated with “L”.